

Midodrine hydrochloride Form A, $C_{12}H_{19}N_2O_4^+ \cdot Cl^-$

Jacob K. Salazar,^a James A. Kaduk,^{b,c,*} Anja Dosen^d and Thomas N. Blanton^d

^aNorth Central College, Department of Chemistry, 131 S. Loomis St., Naperville, IL 60540, USA, ^bNorth Central College, Department of Physics, 131 S. Loomis St., Naperville, IL 60540, USA, ^cIllinois Institute of Technology, Department of Chemistry, 3101 S. Dearborn St., Chicago, IL 60616, USA, and ^dICDD, 12 Campus Blvd., Newtown Square, PA 19073-3273, USA. *Correspondence e-mail: kaduk@polycrystallography.com

Received 23 April 2026

Accepted 8 May 2026

Edited by S.-L. Zheng, Harvard University, USA

Keywords: powder diffraction; midodrine; ProAmatine®; Rietveld refinement; density functional theory.

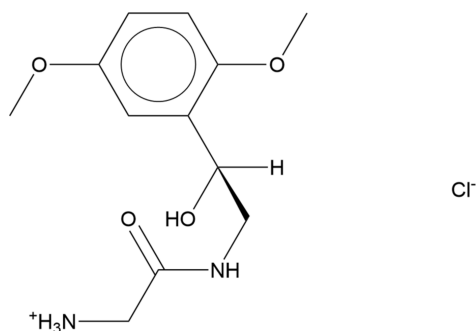
CCDC references: 2552708; 2552707

Supporting information: this article has supporting information at journals.iucr.org/e

The crystal structure of midodrine hydrochloride Form A (systematic name: {[2-(2,5-dimethoxyphenyl)-2-hydroxyethyl]carbamoyl}methanaminium chloride, $C_{12}H_{19}N_2O_4^+ \cdot Cl^-$) has been solved and refined using synchrotron X-ray powder diffraction data, and optimized using density functional theory techniques. Midodrine hydrochloride Form A crystallizes in space group $P2_1/c$ (#14). The crystal structure is characterized by layers perpendicular to the c -axis direction. The Cl anions reside in the center of the layer. Hydrogen bonds are prominent in the structure. Each of the three H on the protonated N acts as a donor – one to the carbonyl group and the other two to the Cl ion. The hydroxyl group and the amide also act as donors to Cl. Considering the classical hydrogen bonds, the Cl ion is four-coordinate.

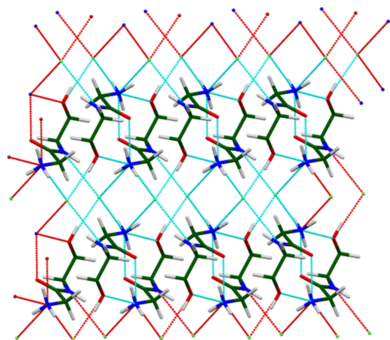
1. Chemical context

Midodrine hydrochloride (marketed as ProAmatine, among others) is used to treat hypotension (low blood pressure) and urinary incontinence. In particular, midodrine HCl treats symptomatic low blood pressure upon standing from a sitting or laying down position. The systematic name (CAS Registry Number 43218-56-0) is 2-amino-*N*-[2-(2,5-dimethoxyphenyl)-2-hydroxyethyl]acetamide hydrochloride.



A process for preparing midodrine hydrochloride has been claimed in US Patent Application US 2022/0144754 A1 (Singh *et al.*, 2022; Cadila Healthcare Ltd.), and powder diffraction data labeled as Form A are provided but no crystal structure was reported.

This work was carried out as part of a project (Kaduk *et al.*, 2014) to determine the crystal structures of large-volume commercial pharmaceuticals, and includes high-quality powder diffraction data for them in the Powder Diffraction File (Kabekkodu *et al.*, 2024).



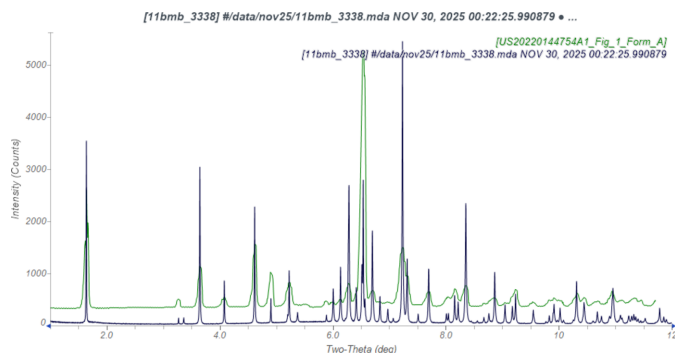


Figure 1
Comparison of the synchrotron pattern from this study of midodrine hydrochloride (black) to that reported for Form A by Singh *et al.* (2022; green). The patent pattern (measured using Cu K_{α} radiation) was digitized using *UN-SCAN-IT* (Silk Scientific, 2013) and converted to the synchrotron wavelength of 0.4687342 Å using *JADE Pro* (MDI, 2026). Image generated using *JADE Pro* (MDI, 2026).

2. Structural commentary

The synchrotron pattern of midodrine hydrochloride is similar enough to that reported by Singh *et al.* (2022) for Form A (Fig. 1) to conclude that they represent the same material. The patent pattern exhibits small displacement/transparency peak position error, as well as significant preferred orientation.

The root-mean-square deviation of the non-H atoms in the Rietveld-refined and *VASP*-optimized structures of midodrine hydrochloride Form A, calculated using the *Mercury* CSD-Materials/Search/Crystal Packing Similarity tool (Macrae *et al.*, 2020) is 0.050 Å (Fig. 2); the structures are essentially identical. The root-mean-square Cartesian displacement of the non-H atoms in the refined and optimized structures of the

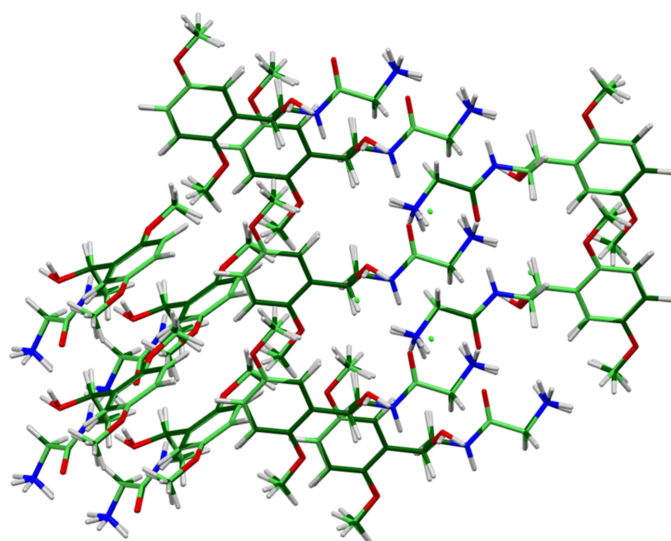


Figure 2
Comparison of the Rietveld-refined (colored by atom type) and *VASP*-optimized (pale green) structures of midodrine hydrochloride Form A, calculated using the *Mercury* CSD-Materials/Search/Crystal Packing Similarity tool. The root-mean-square Cartesian displacement is 0.050 Å. Image generated using *Mercury* (Macrae *et al.*, 2020).

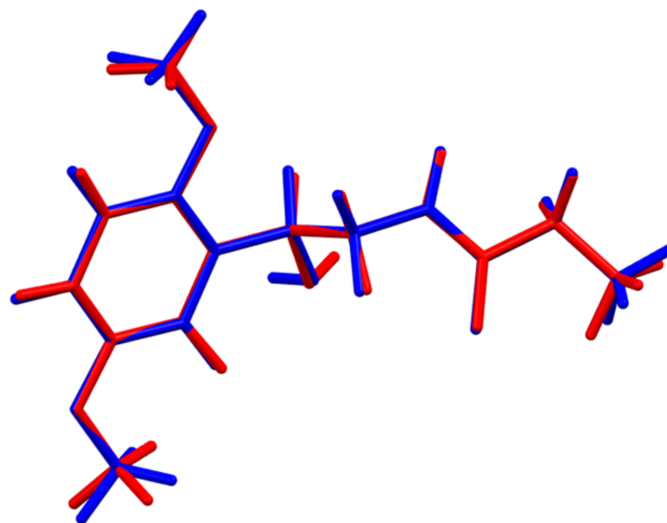


Figure 3
Comparison of the refined structure of the cation in midodrine hydrochloride Form A (red) to the *VASP*-optimized structure (blue). The comparison was generated using the *Mercury* Calculate/Molecule Overlay tool; the r.m.s. deviation is 0.042 Å. Image generated using *Mercury* (Macrae *et al.*, 2020).

cation, calculated using the *Mercury* Calculate/Molecule Overlay tool, is 0.042 Å (Fig. 3). The absolute position difference of the Cl is 0.033 Å. The agreements are within the normal range for correct structures (van de Streek & Neumann, 2014). The asymmetric unit is illustrated in Fig. 4. The remaining discussion will emphasize the *VASP*-optimized structure.

All of the bond distances, bond angles, and torsion angles (Table 1) fall within the normal ranges indicated by a *Mercury* Mogul Geometry check (Macrae *et al.*, 2020). Quantum chemical geometry optimization of the isolated midodrine cation (DFT/B3LYP/6-31G*/water) using *Spartan '24* (Wave-

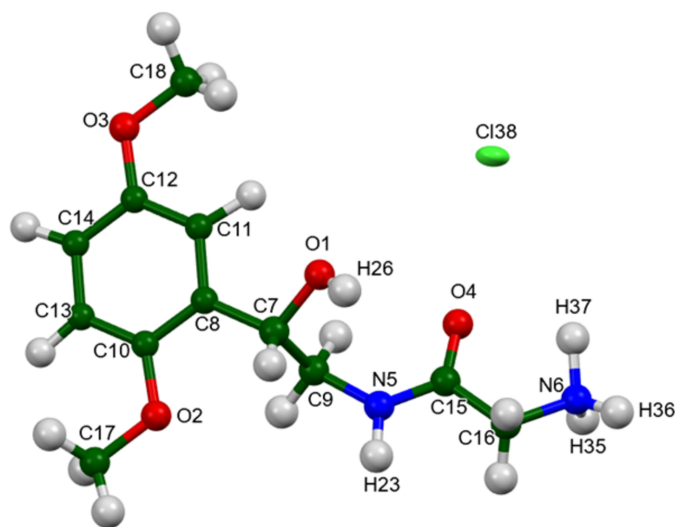


Figure 4
The asymmetric unit of midodrine hydrochloride Form A, with the atom numbering. The atoms are represented by 50% probability spheroids/ellipsoids. Image generated using *Mercury* (Macrae *et al.*, 2020).

Table 1
Selected geometric parameters (Å, °) for midodrine.

O1—C7	1.437 (2)	C15—O4	1.224 (2)
O1—H26	0.989 (2)	C15—N5	1.329 (2)
O2—C10	1.3741 (17)	C15—C16	1.5115 (19)
O2—C17	1.427 (3)	C16—N6	1.467 (3)
O3—C12	1.3814 (19)	C16—C15	1.5115 (19)
O3—C18	1.425 (3)	C16—H27	1.085 (3)
O4—C15	1.224 (2)	C16—H28	1.125 (3)
N5—C9	1.451 (2)	C17—O2	1.427 (3)
N5—C15	1.329 (2)	C17—H29	1.060 (3)
N5—H23	1.047 (2)	C17—H30	1.115 (3)
N6—C16	1.467 (3)	C17—H31	1.100 (3)
N6—H35	1.072 (3)	C18—O3	1.425 (3)
N6—H36	1.070 (2)	C18—H32	1.142 (3)
N6—H37	1.015 (3)	C18—H33	1.067 (3)
C7—O1	1.437 (2)	C18—H34	1.089 (3)
C7—C8	1.5181 (10)	H19—C7	1.118 (3)
C7—C9	1.519 (3)	H20—C9	1.116 (3)
C7—H19	1.118 (3)	H21—C9	1.121 (3)
C8—C7	1.5181 (10)	H22—C11	1.0811 (19)
C8—C10	1.3914 (18)	H23—N5	1.047 (2)
C8—C11	1.4010 (18)	H24—C13	1.119 (2)
C9—N5	1.451 (2)	H25—C14	1.1036 (19)
C9—C7	1.519 (3)	H26—O1	0.989 (2)
C9—H20	1.116 (3)	H26—Cl38 ^d	2.1733 (10)
C9—H21	1.121 (3)	H27—C16	1.085 (3)
C10—O2	1.3741 (17)	H28—C16	1.125 (3)
C10—C8	1.3914 (18)	H29—C17	1.060 (3)
C10—C13	1.391 (2)	H30—C17	1.115 (3)
C11—C8	1.4010 (18)	H31—C17	1.100 (3)
C11—C12	1.3917 (18)	H32—C18	1.142 (3)
C11—H22	1.0811 (19)	H33—C18	1.067 (3)
C12—O3	1.3814 (19)	H34—C18	1.089 (3)
C12—C11	1.3917 (18)	H35—N6	1.072 (3)
C12—C14	1.383 (2)	H35—Cl38 ⁱⁱ	2.1656 (10)
C13—C10	1.391 (2)	H36—N6	1.070 (2)
C13—C14	1.378 (2)	H36—Cl38 ⁱⁱⁱ	2.0529 (10)
C13—H24	1.119 (2)	H37—N6	1.015 (3)
C14—C12	1.383 (2)	C138—H26 ^f	2.1733 (10)
C14—C13	1.378 (2)	C138—H35 ⁱⁱ	2.1656 (10)
C14—H25	1.1036 (19)	C138—H36 ^v	2.0529 (10)
C7—O1—H26	104.5 (2)	C12—C11—H22	122.58 (19)
C10—O2—C17	118.16 (15)	O3—C12—C11	123.4 (2)
C12—O3—C18	118.2 (2)	O3—C12—C14	116.5 (2)
C9—N5—C15	123.69 (18)	C11—C12—C14	120.08 (12)
C9—N5—H23	117.7 (2)	C10—C13—C14	120.27 (14)
C15—N5—H23	117.5 (2)	C10—C13—H24	120.83 (18)
C16—N6—H35	108.7 (2)	C14—C13—H24	118.9 (2)
C16—N6—H36	109.0 (2)	C12—C14—C13	120.11 (13)
H35—N6—H36	104.9 (2)	C12—C14—H25	119.3 (2)
C16—N6—H37	111.8 (3)	C13—C14—H25	120.6 (2)
H35—N6—H37	111.9 (2)	O4—C15—N5	124.03 (18)
H36—N6—H37	110.3 (2)	O4—C15—C16	120.44 (17)
O1—C7—C8	111.60 (16)	N5—C15—C16	115.28 (18)
O1—C7—C9	107.8 (2)	N6—C16—C15	110.65 (17)
C8—C7—C9	111.2 (2)	N6—C16—H27	107.5 (3)
O1—C7—H19	113.5 (2)	C15—C16—H27	113.1 (3)
C8—C7—H19	106.94 (18)	N6—C16—H28	109.3 (3)
C9—C7—H19	105.68 (19)	C15—C16—H28	109.6 (3)
C7—C8—C10	120.30 (12)	H27—C16—H28	106.7 (2)
C7—C8—C11	120.84 (13)	O2—C17—H29	112.0 (2)
C10—C8—C11	118.84 (11)	O2—C17—H30	111.8 (3)
N5—C9—C7	112.7 (2)	H29—C17—H30	111.3 (3)
N5—C9—H20	107.4 (2)	O2—C17—H31	112.3 (3)
C7—C9—H20	109.9 (2)	H29—C17—H31	106.1 (3)
N5—C9—H21	109.7 (2)	H30—C17—H31	102.9 (2)
C7—C9—H21	110.8 (2)	O3—C18—H32	109.9 (3)
H20—C9—H21	106.0 (2)	O3—C18—H33	107.7 (3)
O2—C10—C8	115.41 (11)	H32—C18—H33	108.8 (3)
O2—C10—C13	124.17 (13)	O3—C18—H34	111.0 (3)
C8—C10—C13	120.42 (12)	H32—C18—H34	106.7 (2)
C8—C11—C12	120.22 (13)	H33—C18—H34	112.8 (3)
C8—C11—H22	117.19 (18)		

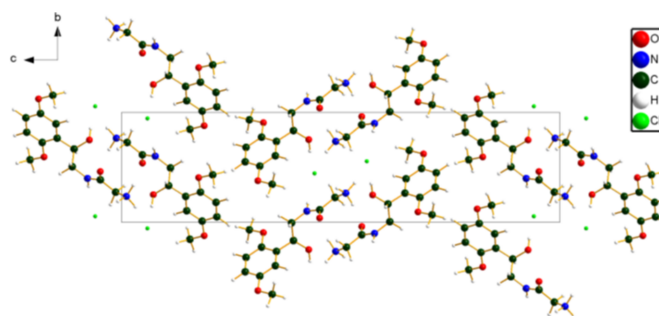


Figure 5
Crystal structure of midodrine hydrochloride Form A, viewed down the *a*-axis. Image generated using *DIAMOND* (Crystal Impact, 2025).

function, 2025) indicated that the observed conformation is 4.4 kcal mol⁻¹ higher in energy than a local minimum, which has an essentially identical conformation (r.m.s. deviation = 0.066 Å). The global minimum-energy conformation (MMFF force field) is 98.1 kcal mol⁻¹ lower in energy, but is unreasonably folded on itself to form intramolecular hydrogen bonds. Intermolecular interactions are important in determining the solid-state conformation.

3. Supramolecular features

The crystal structure (Fig. 5) is characterized by layers perpendicular to the *c*-axis direction. The Cl anions reside in the center of the layer. The *Mercury* Aromatics Analyser indicates three moderate interactions (*d* = 5.18, 5.18, and 6.08 Å), which include both slipped stacking and end-face interactions. The mean plane of the aromatic rings is approximately (3,4,10).

Analysis of the contributions to the total crystal energy of the structure using the Forcite module of *Materials Studio*

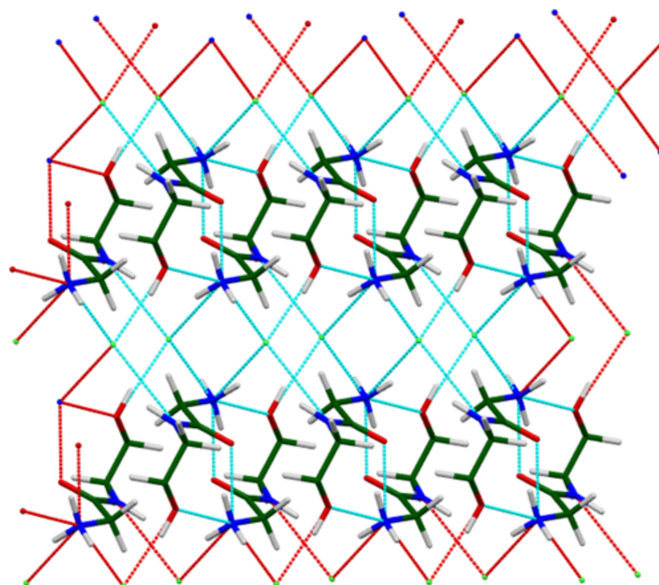


Figure 6
The hydrogen bonding pattern in the layers of midodrine hydrochloride Form A. Image generated using *Mercury* (Macrae *et al.*, 2020).

Table 2
Hydrogen-bond geometry (Å, °).

$D-H\cdots A$	$D-H$	$H\cdots A$	$D\cdots A$	$D-H\cdots A$	Mulliken overlap	H-bond energy
N6—H37···O4	1.043	1.807	2.781	153.7	0.063	5.8
N6—H36···Cl38	1.054	2.070	3.094	163.2	0.088	
N6—H35···Cl38	1.047	2.181	3.159	154.6	0.077	
O1—H26···Cl38	0.993	2.159	3.146	172.1	0.064	35.6
N5—H23···Cl38	1.025	2.545	3.465	149.0	0.036	
C16—H28···Cl38	1.099	2.485	3.422	142.4	0.032	
C11—H22···O1	1.090	2.443	2.825	98.9	0.017	
C13—H24···O3	1.089	2.656	3.592	143.7	0.012	
C17—H31···O3	1.100	2.642	3.637	150.3	0.010	

(Dassault Systèmes, 2025) indicated that the intramolecular energy is dominated by angle distortion terms. The intermolecular energy is small and dominated by van der Waals repulsions, which in this force field based analysis include hydrogen bonds. The hydrogen bonds are better discussed using the results of the DFT calculation.

Hydrogen bonds (Table 2) are prominent in the structure. Each of the three H on the protonated N6 acts as a donor – one to the carbonyl group O4 and the other two to Cl38. The energy of the N—H···O hydrogen bond was calculated using the correlation of Wheatley & Kaduk (2019). The hydroxyl group O1—H26 also acts as a donor to Cl38. The energy of the O—H···Cl bond was calculated using the correlation of Kaduk (2002). The amide N5—H23 also acts as a donor to Cl38. Considering the classical hydrogen bonds, the Cl is four-coordinate. These hydrogen bonds result in rings and chains, with graph sets (Etter, 1990; Bernstein *et al.*, 1995; Motherwell *et al.*, 2000) $R_2^2(10)$, $C_2^1(7)$, $C_2^1(10)$, $R_4^2(20)$, and larger features. The result is a complex network of hydrogen bonds in the center of the layers (Fig. 6). C—H···Cl and C—H···O hydrogen bonds also contribute to the lattice energy.

The volume enclosed by the Hirshfeld surface of midodrine hydrochloride Form A (Fig. 7, Hirshfeld, 1977, Spackman *et*

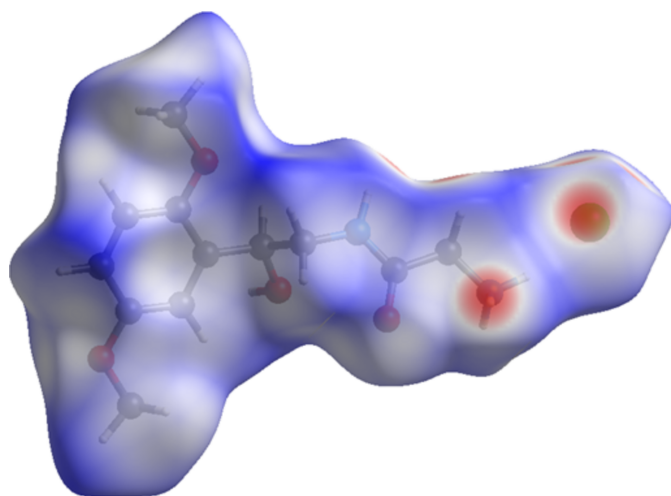


Figure 7
The Hirshfeld surface of midodrine hydrochloride Form A. Intermolecular contacts longer than the sums of the van der Waals radii are colored blue, and contacts shorter than the sums of the radii are colored red. Contacts equal to the sums of radii are white. Image generated using *CrystalExplorer* (Spackman *et al.*, 2021).

al., 2021) is 343.78 \AA^3 , 97.74% of 1/4 of the unit-cell volume. The packing density is thus typical. The close contacts (red in Fig. 7) involve the hydrogen bonds. The volume/non-hydrogen atom is normal, at 18.5 \AA^3 .

The Bravais–Friedel–Donnay–Harker (Bravais, 1866; Friedel, 1907; Donnay & Harker, 1937) algorithm suggests that we might expect platy morphology for midodrine hydrochloride Form A, with {002} as the major faces. A 2nd-order spherical harmonic model for preferred orientation was included. The texture index was 1.003, indicating that the preferred orientation was negligible in this rotated capillary specimen.

4. Database survey

A reduced cell search in the Cambridge Structural Database (CSD 2026.1.0; Groom *et al.*, 2016) yielded 16 hits, but no structures of midodrine or its derivatives.

5. Synthesis and crystallization

Midodrine hydrochloride was a commercial reagent, purchased from TargetMol (Batch #150940), and was used as-received.

6. Refinement

Crystal data, data collection and structure refinement details are summarized in Table 3. The white powder was packed into a 1.5 mm diameter Kapton capillary, and rotated during the measurement at $\sim 50 \text{ Hz}$. The powder pattern was measured at 295 K at beam line 11-BM (Lee *et al.*, 2008; Wang *et al.*, 2008; Antao *et al.*, 2008) of the Advanced Photon Source at Argonne National Laboratory using a wavelength of 0.4687342 \AA from $0.5\text{--}50^\circ 2\theta$ with a step size of 0.001° and a counting time of 0.1 sec/step. The high-resolution powder diffraction data were collected using twelve silicon crystal analyzers that allow for high angular resolution, high precision, and accurate peak positions. A mixture of silicon (NIST SRM 640c) and alumina (NIST SRM 676a) standards (ratio $\text{Al}_2\text{O}_3\text{:Si} = 2\text{:1}$ by weight) was used to calibrate the instrument and refine the monochromatic wavelength used in the experiment.

The pattern was indexed on a primitive monoclinic unit cell with $a = 5.17847$, $b = 8.25254$, $c = 32.94869 \text{ \AA}$, $\beta = 92.757^\circ$, $V =$

Table 3
Experimental details.

midodrine	
Crystal data	
Chemical formula	$C_{12}H_{19}N_2O_4^+Cl^-$
M_r	290.75
Crystal system, space group	Monoclinic, $P2_1/c$
Temperature (K)	295
a, b, c (Å)	5.17893 (2), 8.25455 (3), 32.95227 (15)
β (°)	87.2465 (3)
V (Å ³)	1407.08 (1)
Z	4
Radiation type	Synchrotron, $\lambda = 0.46873$ Å
μ (mm ⁻¹)	0.03
Specimen shape, size (mm)	Cylinder, 2.0 × 1.5
Data collection	
Diffraction	11-BM, APS
Specimen mounting	Kapton capillary
Data collection mode	Transmission
Scan method	Step
2θ values (°)	$2\theta_{\min} = 0.510$, $2\theta_{\max} = 49.995$, $2\theta_{\text{step}} = 0.001$
Refinement	
R factors and goodness of fit	$R_p = 0.049$, $R_{wp} = 0.061$, $R_{exp} = 0.044$, $R(F^2) = 0.03133$, $\chi^2 = 2.008$
No. of parameters	96
No. of restraints	42
$(\Delta/\sigma)_{\max}$	8.514

Computer programs: *GSAS-II* (Toby & Von Dreele, 2013).

1406.4 Å³, and $Z = 4$ using *N-TREOR* as incorporated into *EXPO2014* (Altomare *et al.*, 2013). The suggested space group was $P2_1/c$, which was confirmed by the successful solution and refinement of the structure.

The molecular structure of midodrine was downloaded from PubChem (Kim *et al.*, 2023) as Conformer3D_COMPOUND_CID_4195.sdf. It was converted to a *.mol2 file using *Mercury* (Macrae *et al.*, 2020), and to a Fenske–Hall Z -matrix using *OpenBabel* (O’Boyle *et al.*, 2011). The structure was solved by parallel tempering techniques as implemented in *FOX* (Favre-Nicolin & Černý, 2002) using a midodrine molecule and a Cl atom as fragments, and by Monte Carlo simulated annealing techniques as implemented in *EXPO2014* (Altomare *et al.*, 2013) and *DASH* (David *et al.*, 2006). All three programs yielded equivalent structures. The *FOX* structure was selected for refinement. H37 was added to N6 using *Mercury*.

Rietveld refinement was carried out using *GSAS-II* (Toby & Von Dreele, 2013). Only the 1.5–28.0° portion of the pattern was included in the refinements ($d_{\min} = 0.969$ Å). All non-H bond distances and angles were subjected to restraints, based on a *Mercury*/Mogul Geometry Check (Sykes *et al.*, 2011; Bruno *et al.*, 2004). The Mogul average and standard deviation for each quantity were used as the restraint parameters. The phenyl ring was restrained to be planar. The restraints contributed 1.5% to the overall χ^2 . The hydrogen atoms were included in calculated positions, which were recalculated during the refinement using *Materials Studio* (Dassault Systèmes, 2025). The U_{iso} of the non-H atoms were grouped by chemical similarity. The U_{iso} of the H atoms were fixed at 1.2 ×

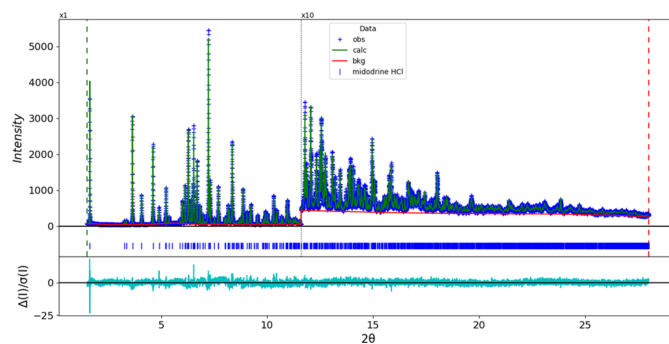


Figure 8

The Rietveld plot for midodrine hydrochloride Form A. The blue crosses represent the observed data points, and the green line is the calculated pattern. The cyan curve is the normalized error plot, and the red line is the background curve. The blue tick marks indicate the peak positions. The vertical scale has been multiplied by a factor of 10× for $2\theta > 11.6^\circ$.

the U_{iso} of the heavy atom to which they are attached. The Cl was refined anisotropically. The peak profiles were described using the generalized microstrain model (Stephens, 1999). The background was modeled using a six-term shifted Chebyshev polynomial, with peaks at 1.58 and 5.56° to model the scattering from the Kapton capillary and any amorphous component of the sample.

The final refinement of 96 variables using 26,501 observations and 42 restraints yielded the residuals $R_{wp} = 0.06154$ and $GOF = 1.42$. The largest peak (0.77 Å from O3) and hole (0.37 Å from O3) in the difference-Fourier map were 0.17 (4) and -0.17 (4) e Å⁻³, respectively. The final Rietveld plot is shown in Fig. 8. The largest features in the normalized error plot are in the shapes of some of the strong low-angle peaks.

The crystal structure of midodrine hydrochloride Form A was optimized (fixed experimental unit cell) with density functional theory techniques using *VASP* (Kresse & Furthmüller, 1996) through the *MedeA* graphical interface (Materials Design, 2024). The calculation was carried out on 32 cores of a 144-core (768 Gb memory) HPE Superdome Flex 280 Linux server at North Central College. The calculation used the GGA-PBE functional, a plane wave cutoff energy of 400.0 eV, and a k -point spacing of 0.5 Å⁻¹ leading to a 3 × 2 × 1 mesh, and took ~2.6 h. Single-point density functional theory calculations (fixed experimental cell) and population analysis were carried out using *CRYSTAL23* (Erba *et al.*, 2023) and *CRYSTAL17* (Dovesi *et al.*, 2018). The basis sets for the H, C, N and O atoms in the calculation were those of Gatti *et al.* (1994), and that for Cl was from Peintinger *et al.* (2013). The calculations were run on a 3.5 GHz PC using 8 k -points and the B3LYP functional, and took ~1.8 hr. The powder pattern has been submitted to ICDD for inclusion in the Powder Diffraction File[®] (PDF[®]).

Acknowledgements

Use of the Advanced Photon Source at Argonne National Laboratory was supported by the US Department of Energy, Office of Science, Office of Basic Energy Sciences, under Contract No. DE-AC02-06CH11357. We thank Saul Lapidus

for his assistance in the data collection. We also thank the ICDD team – Megan Rost, Steve Trimble, and Dave Bohnenberger – for their contribution to research, sample preparation, and in-house XRD data collection and verification.

Funding information

Funding for this research was provided by: International Centre for Diffraction Data (grant No. 09-03).

References

- Altomare, A., Cuocci, C., Giacobuzzo, C., Moliterni, A., Rizzi, R., Corriero, N. & Falcicchio, A. (2013). *J. Appl. Cryst.* **46**, 1231–1235.
- Antao, S. M., Hassan, I., Wang, J., Lee, P. L. & Toby, B. H. (2008). *Can. Mineral.* **46**, 1501–1509.
- Bernstein, J., Davis, R. E., Shimon, L. & Chang, N. L. (1995). *Angew. Chem. Int. Ed. Engl.* **34**, 1555–1573.
- Bravais, A. (1866). *Etudes Cristallographiques*. Paris: Gauthier Villars.
- Bruno, I. J., Cole, J. C., Kessler, M., Luo, J., Motherwell, W. D. S., Purkis, L. H., Smith, B. R., Taylor, R., Cooper, R. I., Harris, S. E. & Orpen, A. G. (2004). *J. Chem. Inf. Comput. Sci.* **44**, 2133–2144.
- Crystal Impact. (2025). *DIAMOND*. Crystal Impact GbR, Bonn, Germany.
- Dassault Systèmes. (2025). *BIOVIA Materials Studio 2025*. BIOVIA, San Diego, CA, USA.
- David, W. I. F., Shankland, K., van de Streek, J., Pidcock, E., Motherwell, W. D. S. & Cole, J. C. (2006). *J. Appl. Cryst.* **39**, 910–915.
- Donnay, J. D. H. & Harker, D. (1937). *Am. Mineral.* **22**, 446–467.
- Dovesi, R., Erba, A., Orlando, R., Zicovich-Wilson, C. M., Civalleri, B., Maschio, L., Rérat, M., Casassa, S., Baima, J., Salustro, S. & Kirtman, B. (2018). *WIREs Comput. Mol. Sci.* **8**, e1360.
- Erba, A., Desmarais, J. K., Casassa, S., Civalleri, B., Donà, L., Bush, I. J., Searle, B., Maschio, L., Edith-Daga, L., Cossard, A., Ribaldone, C., Ascricchi, E., Marana, N. L., Flament, J.-P. & Kirtman, B. (2023). *J. Chem. Theory Comput.* **19**, 6891–6932.
- Etter, M. C. (1990). *Acc. Chem. Res.* **23**, 120–126.
- Favre-Nicolin, V. & Černý, R. (2002). *J. Appl. Cryst.* **35**, 734–743.
- Friedel, G. (1907). *Bull. Soc. Française Minéral.* **30**, 326–455.
- Gatti, C., Saunders, V. R. & Roetti, C. (1994). *J. Chem. Phys.* **101**, 10686–10696.
- Groom, C. R., Bruno, I. J., Lightfoot, M. P. & Ward, S. C. (2016). *Acta Cryst.* **B72**, 171–179.
- Hirshfeld, F. L. (1977). *Theor. Chim. Acta* **44**, 129–138.
- Kabekkodu, S., Dosen, A. & Blanton, T. N. (2024). *Powder Diffr.* **39**, 47–59.
- Kaduk, J. A. (2002). *Acta Cryst.* **B58**, 370–379.
- Kaduk, J. A., Crowder, C. E., Zhong, K., Fawcett, T. G. & Suchomel, M. R. (2014). *Powder Diffr.* **29**, 269–273.
- Kim, S., Chen, J., Cheng, T., Gindulyte, A., He, J., He, S., Li, Q., Shoemaker, B. A., Thiessen, P. A., Yu, B., Zaslavsky, L., Zhang, J. & Bolton, E. E. (2023). *Nucleic Acids Res.* **51**, D1373–D1380.
- Kresse, G. & Furthmüller, J. (1996). *Comput. Mater. Sci.* **6**, 15–50.
- Lee, P. L., Shu, D., Ramanathan, M., Preissner, C., Wang, J., Beno, M. A., Von Dreele, R. B., Ribaud, L., Kurtz, C., Antao, S. M., Jiao, X. & Toby, B. H. (2008). *J. Synchrotron Rad.* **15**, 427–432.
- Macrae, C. F., Sovago, I., Cottrell, S. J., Galek, P. T. A., McCabe, P., Pidcock, E., Platings, M., Shields, G. P., Stevens, J. S., Towler, M. & Wood, P. A. (2020). *J. Appl. Cryst.* **53**, 226–235.
- Materials Design. (2024). *Medea* Version 3.7.2. Materials Design Inc., San Diego, USA.
- MDI (2026). *JADE Pro*. Version 9.5. Materials Data, Livermore, USA.
- Motherwell, W. D. S., Shields, G. P. & Allen, F. H. (2000). *Acta Cryst.* **B56**, 857–871.
- O’Boyle, N. M., Banck, M., James, C. A., Morley, C., Vandermeersch, T. & Hutchison, G. R. (2011). *J. Cheminform* **3**, 33.
- Peintinger, M. F., Oliveira, D. V. & Bredow, T. (2013). *J. Comput. Chem.* **34**, 451–459.
- Silk Scientific. (2013). *UN-SCAN-IT*. Version 7.0. Silk Scientific Corporation, Orem, USA.
- Singh, K. K., Desai, S. J. V. T. P. & Rupapara, M. L. (2022). United States Patent Application US 2022/0144754 A1.
- Spackman, P. R., Turner, M. J., McKinnon, J. J., Wolff, S. K., Grimwood, D. J., Jayatilaka, D. & Spackman, M. A. (2021). *J. Appl. Cryst.* **54**, 1006–1011.
- Stephens, P. W. (1999). *J. Appl. Cryst.* **32**, 281–289.
- Streek, J. van de & Neumann, M. A. (2014). *Acta Cryst.* **B70**, 1020–1032.
- Sykes, R. A., McCabe, P., Allen, F. H., Battle, G. M., Bruno, I. J. & Wood, P. A. (2011). *J. Appl. Cryst.* **44**, 882–886.
- Toby, B. H. & Von Dreele, R. B. (2013). *J. Appl. Cryst.* **46**, 544–549.
- Wang, J., Toby, B. H., Lee, P. L., Ribaud, L., Antao, S. M., Kurtz, C., Ramanathan, M., Von Dreele, R. B. & Beno, M. A. (2008). *Rev. Sci. Instrum.* **79**, 085105.
- Wavefunction (2025). *Spartan ’24*. Version 1.3.1. Wavefunction Inc., Irvine, USA.
- Wheatley, A. M. & Kaduk, J. A. (2019). *Powder Diffr.* **34**, 35–43.

supporting information

Acta Cryst. (2026). E82, 645-650 [https://doi.org/10.1107/S2056989026004810]

Midodrine hydrochloride Form A, $C_{12}H_{19}N_2O_4^+ \cdot Cl^-$

Jacob K. Salazar, James A. Kaduk, Anja Dosen and Thomas N. Blanton

Computing details

{[2-(2,5-Dimethoxyphenyl)-2-hydroxyethyl]carbamoyl}methanaminium chloride (midodrine)

Crystal data

$C_{12}H_{19}N_2O_4^+ \cdot Cl^-$	$V = 1407.08 (1) \text{ \AA}^3$
$M_r = 290.75$	$Z = 4$
Monoclinic, $P2_1/c$	$D_x = 1.373 \text{ Mg m}^{-3}$
$a = 5.17893 (2) \text{ \AA}$	Synchrotron radiation, $\lambda = 0.46873 \text{ \AA}$
$b = 8.25455 (3) \text{ \AA}$	$\mu = 0.03 \text{ mm}^{-1}$
$c = 32.95227 (15) \text{ \AA}$	$T = 295 \text{ K}$
$\beta = 87.2465 (3)^\circ$	cylinder, $2.0 \times 1.5 \text{ mm}$

Data collection

11-BM, APS diffractometer	Data collection mode: transmission
Specimen mounting: Kapton capillary	Scan method: step
	$2\theta_{\min} = 0.510^\circ$, $2\theta_{\max} = 49.995^\circ$, $2\theta_{\text{step}} = 0.001^\circ$

Refinement

Least-squares matrix: full	42 restraints
$R_p = 0.049$	34 constraints
$R_{wp} = 0.061$	Weighting scheme based on measured s.u.'s
$R_{exp} = 0.044$	$(\Delta/\sigma)_{\max} = 8.514$
$R(F^2) = 0.03133$	Background function: Background function:
49486 data points	"chebyshev-1" function with 6 terms: 35.73(7),
Profile function: Finger-Cox-Jephcoat function	-4.92(12), -6.39(12), 3.98(12), -3.39(9),
parameters U, V, W, X, Y, SH/L: peak	-0.15(7), Background peak parameters: pos, int,
variance(Gauss) = $U \tan(\text{Th})^2 + V \tan(\text{Th}) + W$:	sig, gam: 1.580(20), 4.39(21)e3, 2.09(13)e3,
peak HW(Lorentz) = $X/\cos(\text{Th}) + Y \tan(\text{Th})$;	0.100, 5.557(6), 4.34(6)e3, 2.74(7)e3, 0.100,
SH/L = S/L+H/L U, V, W in (centideg) ² , X & Y	Preferred orientation correction: Simple
in centideg 1.163, -0.126, 0.063, 0.000, 0.000,	spherical harmonic correction Order = 2
0.002,	Coefficients: 0:0:C(2,-2) = -0.0581(18);
96 parameters	0:0:C(2,0) = 0.078(4); 0:0:C(2,2) = -0.0919(24)

Fractional atomic coordinates and isotropic or equivalent isotropic displacement parameters (\AA^2)

	x	y	z	$U_{\text{iso}}^*/U_{\text{eq}}$
O1	1.0970 (4)	0.7465 (3)	0.57295 (6)	0.0323 (4)*
O2	0.6632 (4)	0.9002 (2)	0.67443 (6)	0.0391 (5)*
O3	1.3249 (4)	0.3806 (2)	0.68910 (6)	0.0391 (5)*
O4	1.5002 (4)	1.0459 (3)	0.54902 (6)	0.0323 (4)*
N5	1.0987 (4)	1.0938 (3)	0.57585 (7)	0.0323 (4)*

N6	1.4661 (5)	1.2607 (3)	0.48827 (8)	0.0323 (4)*
C7	0.9770 (5)	0.8305 (3)	0.60708 (6)	0.0323 (4)*
C8	0.9847 (5)	0.7310 (3)	0.64575 (6)	0.0311 (5)*
C9	1.1161 (5)	0.9912 (3)	0.61138 (8)	0.0323 (4)*
C10	0.8228 (5)	0.7694 (3)	0.67930 (6)	0.0311 (5)*
C11	1.1581 (5)	0.6018 (3)	0.64869 (7)	0.0311 (5)*
C12	1.1601 (5)	0.5099 (3)	0.68409 (8)	0.0311 (5)*
C13	0.8299 (6)	0.6787 (3)	0.71481 (7)	0.0311 (5)*
C14	0.9978 (6)	0.5498 (3)	0.71712 (7)	0.0311 (5)*
C15	1.2919 (5)	1.1156 (4)	0.54837 (8)	0.0323 (4)*
C16	1.2304 (5)	1.2225 (4)	0.51286 (9)	0.0323 (4)*
C17	0.4688 (6)	0.9328 (4)	0.70550 (9)	0.0391 (5)*
C18	1.5119 (6)	0.3451 (4)	0.65719 (9)	0.0391 (5)*
H19	0.76985	0.86202	0.60297	0.0388 (5)*
H20	1.32549	0.96936	0.61586	0.0388 (5)*
H21	1.04032	1.05789	0.63909	0.0388 (5)*
H22	1.28492	0.57675	0.62242	0.0373 (6)*
H23	0.93892	1.17104	0.57467	0.0388 (5)*
H24	0.70477	0.71120	0.74223	0.0373 (6)*
H25	1.00097	0.47574	0.74497	0.0373 (6)*
H26	0.98954	0.64869	0.56984	0.0388 (5)*
H27	1.09480	1.16753	0.49287	0.0388 (5)*
H28	1.13894	1.33833	0.52442	0.0388 (5)*
H29	0.35462	1.03463	0.69851	0.0469 (6)*
H30	0.34623	0.82426	0.71243	0.0469 (6)*
H31	0.55160	0.95960	0.73490	0.0469 (6)*
H32	1.41042	0.31642	0.62801	0.0469 (6)*
H33	1.61746	0.24085	0.66595	0.0469 (6)*
H34	1.63568	0.44937	0.65061	0.0469 (6)*
H35	1.60707	1.30873	0.50782	0.0388 (5)*
H36	1.42630	1.35768	0.46795	0.0388 (5)*
H37	1.53415	1.16293	0.47244	0.0388 (5)*
Cl38	0.2652 (2)	0.55463 (11)	0.44075 (3)	0.0394

Atomic displacement parameters (Å²)

	U^{11}	U^{22}	U^{33}	U^{12}	U^{13}	U^{23}
Cl38	0.0457 (9)	0.0273 (9)	0.0446 (9)	0.0127 (16)	0.0036 (15)	-0.0002 (15)

Geometric parameters (Å, °)

O1—C7	1.437 (2)	C15—O4	1.224 (2)
O1—H26	0.989 (2)	C15—N5	1.329 (2)
O2—C10	1.3741 (17)	C15—C16	1.5115 (19)
O2—C17	1.427 (3)	C16—N6	1.467 (3)
O3—C12	1.3814 (19)	C16—C15	1.5115 (19)
O3—C18	1.425 (3)	C16—H27	1.085 (3)
O4—C15	1.224 (2)	C16—H28	1.125 (3)

N5—C9	1.451 (2)	C17—O2	1.427 (3)
N5—C15	1.329 (2)	C17—H29	1.060 (3)
N5—H23	1.047 (2)	C17—H30	1.115 (3)
N6—C16	1.467 (3)	C17—H31	1.100 (3)
N6—H35	1.072 (3)	C18—O3	1.425 (3)
N6—H36	1.070 (2)	C18—H32	1.142 (3)
N6—H37	1.015 (3)	C18—H33	1.067 (3)
C7—O1	1.437 (2)	C18—H34	1.089 (3)
C7—C8	1.5181 (10)	H19—C7	1.118 (3)
C7—C9	1.519 (3)	H20—C9	1.116 (3)
C7—H19	1.118 (3)	H21—C9	1.121 (3)
C8—C7	1.5181 (10)	H22—C11	1.0811 (19)
C8—C10	1.3914 (18)	H23—N5	1.047 (2)
C8—C11	1.4010 (18)	H24—C13	1.119 (2)
C9—N5	1.451 (2)	H25—C14	1.1036 (19)
C9—C7	1.519 (3)	H26—O1	0.989 (2)
C9—H20	1.116 (3)	H26—C138 ⁱ	2.1733 (10)
C9—H21	1.121 (3)	H27—C16	1.085 (3)
C10—O2	1.3741 (17)	H28—C16	1.125 (3)
C10—C8	1.3914 (18)	H29—C17	1.060 (3)
C10—C13	1.391 (2)	H30—C17	1.115 (3)
C11—C8	1.4010 (18)	H31—C17	1.100 (3)
C11—C12	1.3917 (18)	H32—C18	1.142 (3)
C11—H22	1.0811 (19)	H33—C18	1.067 (3)
C12—O3	1.3814 (19)	H34—C18	1.089 (3)
C12—C11	1.3917 (18)	H35—N6	1.072 (3)
C12—C14	1.383 (2)	H35—C138 ⁱⁱ	2.1656 (10)
C13—C10	1.391 (2)	H36—N6	1.070 (2)
C13—C14	1.378 (2)	H36—C138 ⁱⁱⁱ	2.0529 (10)
C13—H24	1.119 (2)	H37—N6	1.015 (3)
C14—C12	1.383 (2)	C138—H26 ^j	2.1733 (10)
C14—C13	1.378 (2)	C138—H35 ⁱⁱ	2.1656 (10)
C14—H25	1.1036 (19)	C138—H36 ^{iv}	2.0529 (10)
C7—O1—H26	104.5 (2)	C12—C11—H22	122.58 (19)
C10—O2—C17	118.16 (15)	O3—C12—C11	123.4 (2)
C12—O3—C18	118.2 (2)	O3—C12—C14	116.5 (2)
C9—N5—C15	123.69 (18)	C11—C12—C14	120.08 (12)
C9—N5—H23	117.7 (2)	C10—C13—C14	120.27 (14)
C15—N5—H23	117.5 (2)	C10—C13—H24	120.83 (18)
C16—N6—H35	108.7 (2)	C14—C13—H24	118.9 (2)
C16—N6—H36	109.0 (2)	C12—C14—C13	120.11 (13)
H35—N6—H36	104.9 (2)	C12—C14—H25	119.3 (2)
C16—N6—H37	111.8 (3)	C13—C14—H25	120.6 (2)
H35—N6—H37	111.9 (2)	O4—C15—N5	124.03 (18)
H36—N6—H37	110.3 (2)	O4—C15—C16	120.44 (17)
O1—C7—C8	111.60 (16)	N5—C15—C16	115.28 (18)
O1—C7—C9	107.8 (2)	N6—C16—C15	110.65 (17)

C8—C7—C9	111.2 (2)	N6—C16—H27	107.5 (3)
O1—C7—H19	113.5 (2)	C15—C16—H27	113.1 (3)
C8—C7—H19	106.94 (18)	N6—C16—H28	109.3 (3)
C9—C7—H19	105.68 (19)	C15—C16—H28	109.6 (3)
C7—C8—C10	120.30 (12)	H27—C16—H28	106.7 (2)
C7—C8—C11	120.84 (13)	O2—C17—H29	112.0 (2)
C10—C8—C11	118.84 (11)	O2—C17—H30	111.8 (3)
N5—C9—C7	112.7 (2)	H29—C17—H30	111.3 (3)
N5—C9—H20	107.4 (2)	O2—C17—H31	112.3 (3)
C7—C9—H20	109.9 (2)	H29—C17—H31	106.1 (3)
N5—C9—H21	109.7 (2)	H30—C17—H31	102.9 (2)
C7—C9—H21	110.8 (2)	O3—C18—H32	109.9 (3)
H20—C9—H21	106.0 (2)	O3—C18—H33	107.7 (3)
O2—C10—C8	115.41 (11)	H32—C18—H33	108.8 (3)
O2—C10—C13	124.17 (13)	O3—C18—H34	111.0 (3)
C8—C10—C13	120.42 (12)	H32—C18—H34	106.7 (2)
C8—C11—C12	120.22 (13)	H33—C18—H34	112.8 (3)
C8—C11—H22	117.19 (18)		

Symmetry codes: (i) $-x+1, -y+1, -z+1$; (ii) $-x+2, -y+2, -z+1$; (iii) $x+1, y+1, z$; (iv) $x-1, y-1, z$.

(midodrine_midodrine_VASP)

Crystal data

$C_{12}H_{19}ClN_2O_4$

$M_r = 290.75$

Monoclinic, $P2_1/c$

$a = 5.17880 \text{ \AA}$

$b = 8.25410 \text{ \AA}$

$c = 32.95150 \text{ \AA}$

$\beta = 87.25^\circ$

$V = 1406.93 \text{ \AA}^3$

$Z = 4$

Data collection

$h = \rightarrow$

$k = \rightarrow$

$l = \rightarrow$

Fractional atomic coordinates and isotropic or equivalent isotropic displacement parameters (\AA^2)

	x	y	z	$B_{\text{iso}}^*/B_{\text{eq}}$
O1	1.08609	0.75160	0.57288	
O2	0.66329	0.90588	0.67624	
O3	1.32010	0.37844	0.68884	
O4	1.49956	1.03863	0.54807	
N5	1.10117	1.10119	0.57712	
N6	1.46798	1.26472	0.48858	
C7	0.97486	0.83368	0.60772	
C8	0.98777	0.73521	0.64646	
C9	1.11992	0.99460	0.61196	
C10	0.82320	0.77413	0.68029	
C11	1.15908	0.60486	0.64894	
C12	1.16333	0.51097	0.68431	
C13	0.82942	0.68120	0.71575	

C14	0.99768	0.55011	0.71764
C15	1.28930	1.11376	0.54791
C16	1.23005	1.22586	0.51307
C17	0.47051	0.93180	0.70822
C18	1.50565	0.34561	0.65626
H19	0.76985	0.86202	0.60297
H20	1.32549	0.96936	0.61586
H21	1.04032	1.05789	0.63909
H22	1.28492	0.57675	0.62242
H23	0.93892	1.17104	0.57467
H24	0.70477	0.71120	0.74223
H25	1.00097	0.47574	0.74497
H26	0.98954	0.64869	0.56984
H27	1.09480	1.16753	0.49287
H28	1.13894	1.33833	0.52442
H29	0.35462	1.03463	0.69851
H30	0.34623	0.82426	0.71243
H31	0.55766	0.96164	0.73709
H32	1.41042	0.31642	0.62801
H33	1.61746	0.24085	0.66595
H34	1.63568	0.44937	0.65061
H35	1.60707	1.30873	0.50782
H36	1.42630	1.35768	0.46795
H37	1.53415	1.16293	0.47244
Cl38	1.26072	1.55497	0.44040

Hydrogen-bond geometry (Å, °)

<i>D—H···A</i>	<i>D—H</i>	<i>H···A</i>	<i>D···A</i>	<i>D—H···A</i>
N6—H37···O4	1.043	1.807	2.781	153.7
N6—H36···Cl38	1.054	2.070	3.094	163.2
N6—H35···Cl38	1.047	2.181	3.159	154.6
O1—H26···Cl38	0.993	2.159	3.146	172.1
N5—H23···Cl38	1.025	2.545	3.465	149.0
C16—H28···Cl38	1.099	2.485	3.422	142.4
C11—H22···O1	1.090	2.443	2.825	98.9
C13—H24···O3	1.089	2.656	3.592	143.7
C17—H31···O3	1.100	2.642	3.637	150.3
